Two-step electrical percolation in nematic liquid crystals filled with multiwalled carbon nanotubes

Serhiy Tomylko* and Oleg Yaroshchuk†
Institute of Physics, NAS of Ukraine, Prospect Nauky 46, 03028, Kyiv, Ukraine

Nikolai Lebovka‡
Institute of Biocolloidal Chemistry named after F.D. Ovcharenko, NAS of Ukraine, Prospect Vernadskogo 42, 03142, Kyiv, Ukraine
(Received 28 April 2015; published 7 July 2015)

Percolation of carbon nanotubes (CNTs) in liquid crystals (LCs) opens the way for a unique class of anisotropic hybrid materials with a complex dielectric constant widely controlled by CNT concentration. Percolation in such systems is commonly described as a one-step process starting at a very low loading of CNTs. In the present study the two-step percolation was observed in the samples of thickness 250 μm obtained by pressing the suspension between two substrates. The first threshold concentration, $C_n^{p_1} \sim 10^{-4}$ wt.%, was sensitive to temperature and phase state of LC, while the second one, $C_n^{p_2} \sim 10^{-1}$ wt.%, remained practically unchanged in the temperature tests. The two-stage nature of percolation was explained on a base of mean-field theory assuming core-shell structure of CNTs.

DOI: 10.1103/PhysRevE.92.012502 PACS number(s): 61.30.−v, 61.48.De, 64.60.ah

I. INTRODUCTION

Carbon nanotubes (CNTs) have extraordinarily large shape anisotropy (the length-to-diameter ratio may be as large as 500–1000), high mechanical strength, large anisotropy of electric and thermal conductivity, and high chemical resistance. Different types of electrochemical biosensors, strain sensors, electromagnetic switches, screens and other multifunctional devices made from materials containing CNTs have been proposed [1–5].

Nowadays, liquid crystals (LC) filled by CNTs attract both scientific and practical interest [6–10]. The orientational ordering of LC host imposes ordering of CNTs and has an impact on their aggregation [11,12]. Moreover, the ordering direction of CNTs can be easily controlled by external electric or magnetic field [11,12]. On the other hand, doping of LC by CNTs may essentially improve electro-optic performance of LC cells. It allows for reduction of the response time and driving voltage, as well as suppression of undesirable back flow and image retention [13]. Moreover, the nanotubes bring unusual properties to LCs, such as much enhanced permittivity and electrical conductivity [14] as well as remarkable electro-optical [8] and electromechanical [15] memory effects.

In the majority of previous works, the concentration of CNTs in LC suspension was rather small ($\leqslant 10^{-3}$ wt.%) in order to avoid their essential aggregation. At the same time, increasing of CNT concentration enhances properties of these particles in the composites and leads to a number of exciting features, such as percolation phenomena and accompanying memory effect [8,16–19].

The percolation phenomena in the colloidal systems based on CNTs are caused by three-dimensional continuous networks formed by these particles in the dispersion media at some concentration of CNTs called percolation concentration or percolation point, C_n^p. Usually, this structural process is accompanied by an abrupt increase of electrical conductivity [20] and mechanical rigidity [21] in the vicinity of C_n^p. The value of C_n^p can be controlled by many different factors, such as distribution of quality of electrical contacts or junctions between different particles [22], presence of interfacial shells around particles embedded in the continuous matrix [23], clustering, agglomeration [24] or segregation of particles [25], variation in the shape and orientation of aggregates and local particle concentration [26], dependence of the network structure on the particle concentration [27], and orientational ordering of CNTs inside a matrix [28–31]. As for the last factor, alignment of CNTs can essentially affect percolation characteristics. The high ordering of CNTs destroys the percolation pathways created by intersected nanotubes and thus decreases electrical conductivity. However, Monte Carlo simulations indicate that maximal conductivity can be achieved for slightly aligned rather than isotropically distributed CNTs [32]. This is in good agreement with the increase of electrical conductivity in CNT composites caused by magnetic field [33] or mechanical shear [34].

Fundamentally new opportunities for studying the influence of orientational ordering of CNTs on percolation characteristics are opened when using LC matrices. In contrast to isotropic polymer matrices in which the orientational order is formed under external action like extrusion or shear, this order in LCs occurs spontaneously due to molecular self-assembling. The structure of LC mesophases is rather sensitive to external factors such as heat and electric or magnetic field. Thus ordering of CNTs integrated in LC can easily be tuned by soft acting on the LC host.

Despite such opportunities, experimental data on percolation phenomena in LC-CNTs systems are quite scarce [8,35–37]. They entirely refer to percolation of electric conductivity in thin cells ($d < 20$ μm) and can be reduced to the following conclusions:

(1) The percolation in LCs is essentially a single-step process with a rather low percolation point ($C_n^p \approx 0.01$ wt.%).

(2) The percolation concentration depends on the phase state of the LC medium. In particular, in a nematic phase of 5CB, the percolation point was found to be $C_n^p \approx 0.01$ wt.%,

*tomulkosv@ukr.net
†Corresponding author: o.yaroshchuk@gmail.com
‡lebovka@gmail.com

whereas it noticeably increased up to 0.1 wt.% in the isotropic phase [8].

(3) By reaching the percolation transition, the dominant mechanism of electrical conductivity becomes a charge tunneling and hopping between single nanotubes. The next strengthening of percolation network results in the domination of a mechanism typical for nanotube bundles. These changes in the character of conductivity are explained by improvement of electrical contacts between the percolating nanotubes [8].

These properties are in good agreement with the properties of the percolation transition of CNTs in polymer matrices. The exception makes only the first conclusion consisting in a single-stage nature of the transition. These systems demonstrate fuzzy-type or multiple transitions with two or even more percolation thresholds reflecting different stages of formation of percolation network [25,27,38].

In the present paper, to clarify the nature of the percolation transition in the system LC-CNTs, we analyze more thoroughly the dependence of the electrical conductivity σ on the concentration of nanotubes C_n using different methods of filling of the composites in LC cells. This research helped us to find an optimal method of filling which naturally leads to two-stage percolation typical for the dispersions of CNTs in other matrices. In the following, we analyze this percolation in terms of scaling law and present a model of this process and its simplest mathematical description.

The rest of the paper is constructed as follows. In Sec. II we describe the materials, technical details used for preparation of samples, and methods. Sections III and IV present our main findings. In Sec. V, we summarize the results and conclude the paper.

II. EXPERIMENTAL

A. Materials

The nematic liquid crystal 5CB (Merck) with the nematic-to-isotropic transition at 35.4 °C and the crystal-to-nematic transition at 22.5 °C was used in this study. Entangled multi-walled CNTs were prepared from ethylene using the chemical vapor deposition method (TMSpetsmash Ltd., Kyiv, Ukraine) with Fe-Al-Mo catalyst [39]. CNTs were further purified by alkaline and acidic solutions and washed by distilled water until reaching the distilled water pH and conductivity values in the filtrate. The typical outer diameter of CNTs, estimated from electrical microscopy images, was ≈30 nm, while their length ranged from 10 to 20 μm [40]. The specific surface area of the CNT powder, determined by N_2 adsorption, was 130 ± 5 m^2/g. The specific electric conductivity σ_n of the powder of CNTs compressed at 15 TPa was about 10 S/cm along the axis of compression.

B. Preparation of samples

LCs filled by CNTs were obtained by adding appropriate weights of CNTs ($C_n = 0.025$–2.0 wt.%) to 5CB at $= 60$ °C with subsequent 10-min sonication using an ultrasonic disperser at 22 kHz and 250 W. Then composites were incubated at room temperature for 24 h, sonicated again for 2 min, and loaded into the cells. The volume fraction of CNTs in the composites φ_n was estimated as

$$\varphi_n = [1 + (1/C_n - 1)\rho_n/\rho_0]^{-1} \approx C_n\rho_0/\rho_n \approx 0.5C_n, \quad (1)$$

where ρ_0 and ρ_n are the densities of 5CB and CNTs, respectively. The value of ρ_0 used in this calculation was 1020 kg/m^3 [41]. The density of the CNTs was assumed to be the same as the density of pure graphite, $\rho_n = 2045$ kg/m^3.

Calorimetric studies of the resulting mixtures have not detected the effect of CNTs on the clearing temperature T_c of LC 5CB, which was 35.4 °C.

Two methods were used for loading the composites into the cell:

(1) Filling the composites by capillary forces in the preassembled cells (C cell).

(2) Pressing of small amount of the composite between two substrates forming a cell (P cell).

The cells were made from two glass substrates, containing patterned ITO electrodes and layers of polyimide AL3046 (JSR, Japan) designed for planar alignment. The spin-coated polyimide films were properly backed and rubbed by a fleece cloth in order to provide a uniform planar alignment of LC in the field-off state. The cells were assembled so the rubbing directions of the opposite aligning layers were antiparallel. The cell gap d was maintained by 50- and 250-μm Teflon strips. Cell bonding was performed with an epoxy glue.

C. Methods

The macroscopic alignment in the cells was tested using a light box and two sheet polarizers, while the microstructure was studied using optical polarization microscope Polam L-213M equipped by digital camera conjugated with a personal computer.

The dielectric studies were conducted by use of the oscilloscopic method in the temperature range 25–50 °C. The resistance and capacitance of the LC cells were experimentally measured in a wide frequency range, $f = 10^{-1}$–10^6 Hz and used for calculation of real ϵ' and imaginary ϵ'' parts of complex dielectric constant $\epsilon^* = \epsilon' - i\epsilon''$. The frequency $f =$ 2 kHz from the range $10 < f < 10^4$ Hz free of any relaxation processes was selected for further evaluation of permittivity ϵ' and conductivity σ values corresponding to the bulk part of a sample. The AC conductivity σ was estimated from the formula $\sigma = 2\pi\epsilon_0\epsilon'' f$, where ϵ_0 is the electric permittivity of free space.

D. Statistical analysis

Each measurement was repeated at least 3 times for calculation of the mean values and root-mean-square errors. The error bars in all figures correspond to the confidence level of 95%.

III. RESULTS

Figure 1 compares microphotographs of the 50-μm layers of 5CB-CNT suspensions inserted into the C cells [Fig. 1(a)] and P cells [Fig. 1(b)] with different concentrations of CNTs. It can be seen that the microphotographs are rather similar for C and P cells up to the concentration $C_n \approx 0.05$ wt.%. Above $C_n \approx 0.05$–0.1 wt.%, the method of cell preparation becomes

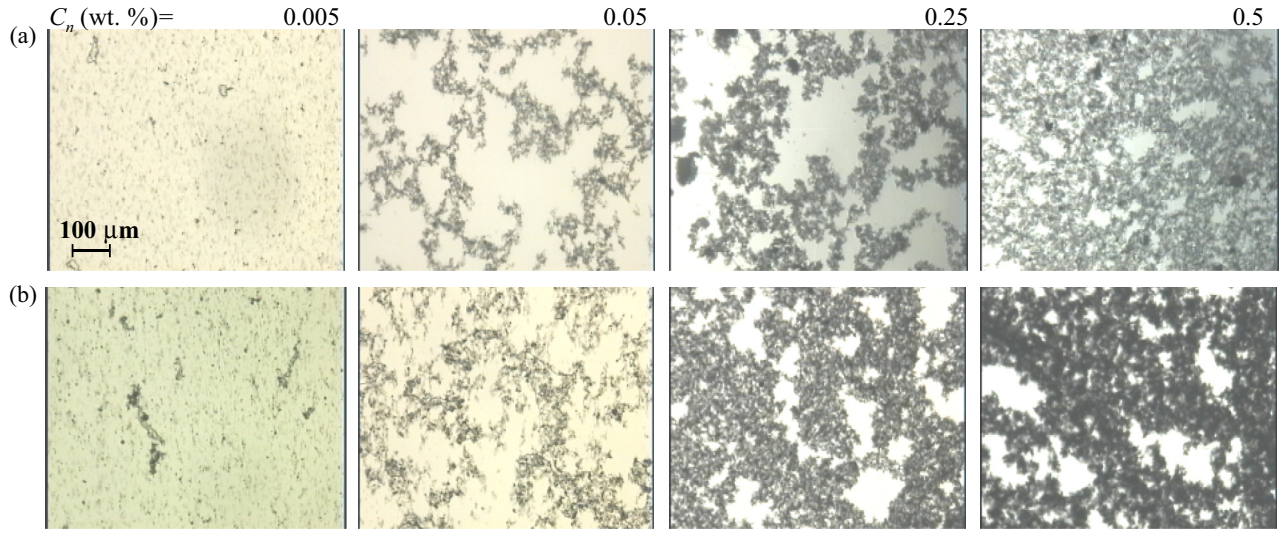

FIG. 1. (Color online) Microphotographs of the layers of 5CB-CNT suspensions filled in the cells with a thickness of 50 μm. Concentration of CNTs in the samples 1, 2, 3, and 4 is 0.005, 0.05, 0.25, and 0.5 wt. %, respectively. Series (a) and (b) correspond, respectively, to C and P series of samples. It is evident that the amount of nanotubes in both series is comparable up to $C_n = 0.05$ wt.% but begins to differ at higher C_n. The data correspond to the nematic phase, $T = 25^{\circ}$C.

quite important. The aggregates in P cells are more compacted as compared with those in corresponding C cells. This fact can be explained by smaller actual concentration of CNTs inside the C cells. Indeed, the concentration of CNTs inside the P cells should be equal to the concentration of CNTs in a bulk suspension, C_n. However, the situation in the C cells differs. When the thickness of the cells d is comparable or smaller than the size of aggregates, only the aggregates with the size smaller than d or individual CNTs are effectively involved by LC subjected to capillary forces in the filling process. It results in selective sampling of CNTs at the edges of the C cell. The filtered-out large aggregates that remained at the entrance to the cell can be easily observed in an optical microscope.

Concentration dependencies of the electrical conductivity of 5CB-CNT composites, $\sigma(C_n)$, in the C and P cells are shown in Fig. 2. Figures 2(a) and 2(b) correspond to thickness of the cells 50 and 250 μm, respectively. Initially, these curves sharply rise and subsequently demonstrate tendency to saturation. The data show that the curves $\sigma(C_n)$ for the C and P series diverge with increasing CNT concentration starting at $C_n \approx 0.05$ wt.% for $d = 50$ μm and $C_n \approx 0.2$ wt.% for $d = 250$ μm, so the measured electrical conductivity in the C cells becomes noticeably smaller than in the P cells. This indicates smaller actual concentration of CNTs inside the C cell, which is in full correspondence with the data of microphotographs presented in Fig. 1. Thus, since the actual concentration of CNTs in the C cells cannot be estimated correctly, the capillary filling is not a suitable method for LC suspensions with enhanced loading of CNTs. Because of this, only the curves corresponding to the P series of samples will further be analyzed.

Figure 2 shows a distinct difference in the $\sigma(C_n)$ curves obtained for the $d = 50$ μm and $d = 250$ μm series of P cells. The $\sigma(C_n)$ curve for $d = 50$ μm demonstrates single-stage growth as in a number of previous studies [8,36,37]. In turn, the curve for the $d = 250$ μm series shows a two-stage percolation character, similarly to many polymer dispersions of CNTs [27,38,42]. Finally, note that this multistage character is not visible for the concentration dependence of effective permittivity. Figure 3 shows that the $\epsilon'(C_n)$ curves monotonically grow with a tendency to saturation and have a smooth shape. The dependencies of $\sigma(C_n)$ and $\epsilon'(C_n)$ obtained for isotropic phase ($T = 55^{\circ}$C) (Figs. 2 and 3) lie above the corresponding curves for the nematic phase ($T = 25^{\circ}$C). This tendency is natural since σ and ϵ' in LC grow with temperature. Qualitatively, the character of the percolation in the isotropic phase is the same as in the nematic phase.

IV. DISCUSSION

We turn first to the sample preparation procedure for the composites LC-CNTs. In the previous studies of these materials the procedure developed for liquid crystals was used. It consisted of the LC being filled up in a thin planar cell by means of capillary forces. As shown above, this procedure is acceptable for low concentrations of CNTs but becomes unreliable with increasing of the concentration. The problem is caused by blocking of bigger aggregates of CNTs at entrance to the cell, which intensifies with a growth of CNT concentration. It is natural that the smaller the thickness of the cell the lower the critical concentration of CNTs at which the efficiency of the method of capillary filling is lost (Fig. 2). The situation aggravates with lengthening and entanglement of nanotubes that promotes their aggregation. On the contrary, the limit of applicability of capillary filling can be significantly increased by using short-length nanotubes. We demonstrated this by using multiwalled CNTs from Cheap Tubes (USA), having a length of 0.5–2 μm. In this case, the critical concentration for capillary filling in 50-μm cells was increased to 0.5 wt.%. The details of these studies will be separately published elsewhere.

After determining conditions for observation of the two-stage electrical percolation, we move on to the specifics of this process. According to Fig. 2(b), the $\sigma(C_n)$ curve demonstrates a sequence of two sharp increases and saturations. This

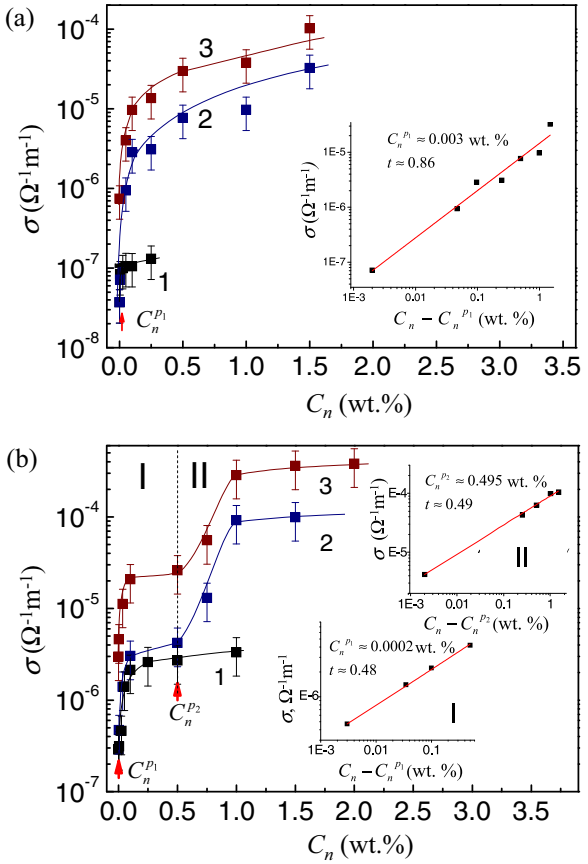

FIG. 2. (Color online) Electrical conductivity σ versus CNT concentration C_n curves for the layers of 5CB-CNT suspensions with a thickness of 50 μm (a) and 250 μm (b). Lines are added to guide the eyes. Curve 1 corresponds to the C series, while curves 2 and 3 correspond to the P series. Temperature of measurements was 25°C for curves 1 and 2 and 55°C for curve 3. The numbers I and II in (b) mark concentration ranges of the first and second percolation processes. The insets present curve 2 (P series, 25°C) or its parts in double logarithmic scale along with the fitting curves according to Eq. (2).

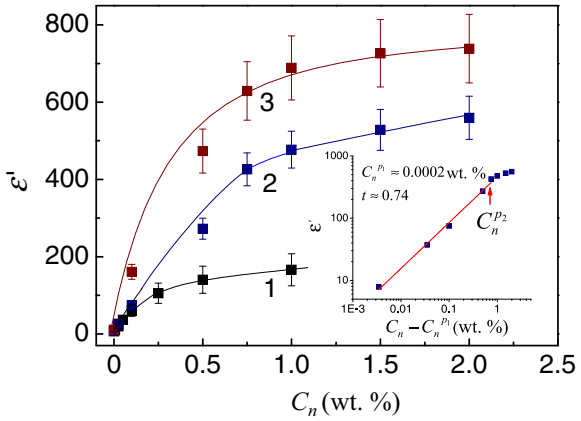

FIG. 3. (Color online) Effective dielectric constant of 5CB-CNT suspension ϵ' as a function of CNT concentration C_n for the samples of thickness 250 μm. Lines are added to guide the eye. Curve 1 corresponds to the C series, while curves 2 and 3 correspond to the P series. The temperatures of the measurements were 25°C for curves 1 and 2 and 55°C for curve 3. The inset represents curve 2 in a double logarithmic scale along with the best fit to it with a function $\epsilon' \propto (C_n - C_n^{p1})$.

two-stage character seems to be a common feature of fluid composites with low viscosity. In particular, it was previously observed for CNT dispersions in polymer matrices. The first percolation process was attributed to dynamic (kinetic) percolation appearing due to movement and interactions of CNTs. It can be described by dynamic theory [20,38]. A rather low value of the threshold concentration observed for this process ($C_n^{p1} = 10^{-3}$–10^{-1} wt.% [20,43]) was explained by the low viscosity of the fluidlike matrix, promoting intensive movement of CNTs and, as result, their flocculation. The same mechanism may explain low-threshold percolation in LC systems, which was a single percolation detected in previous studies and the first percolation in the present research.

Earlier, by working with thinner samples, we believed that a low value of threshold concentration of CNTs in LCs (10^{-3}-10^{-2} wt.%) is caused by the fact that the length of the CNTs is comparable with the thickness of the dispersion layer. This means that even single nanotubes or their small linear aggregates are capable of "short-circuiting" the samples causing seeming percolation. However, the results of the present work demonstrate that threshold concentration of this process does not depend very much on cell thickness and therefore the above-mentioned explanation is no longer convincing. On the contrary, the dynamic nature of network formation explains the low percolation threshold very logically, because nematic LC is a fluid of low viscosity.

The second percolation process in polymer dispersions of CNTs [38] was assigned to static percolation developing at higher loading when Brownian motions of CNTs are restricted. It can be described by statistical theories assuming random particle distribution and absence of their movement and interaction. The $\sigma(C_n)$ curve in this process is usually well fitted to percolation scaling law

$$\sigma \propto \left(C_n - C_n^p\right)^t, \tag{2}$$

where C_n^p and t are percolation concentration and transport exponent, respectively. In Ref. [38], the second percolation point of the $\sigma(C_n)$ curve was observed as a crossover from saturation state achieved after the first percolation to the power-law behavior described by Eq. (2).

In our case, the behavior of the $\sigma(C_n)$ curve differs a bit. Two parts of this curve corresponding to different stages of percolation are qualitatively similar. They consist of rapid growing and saturation sections. The second saturation which was not detected in polymer dispersions of CNTs is probably due to a wider concentration range used in our research. Another feature is that both percolation processes are fitted well to the scaling law described by Eq. (2). This may indicate that dynamic processes play an important role only during formation of the CNT network. At the same time, the network formed even at the first percolation stage is sufficiently stable and can be described within the framework of statistical theories. The fitting parameters for the first and

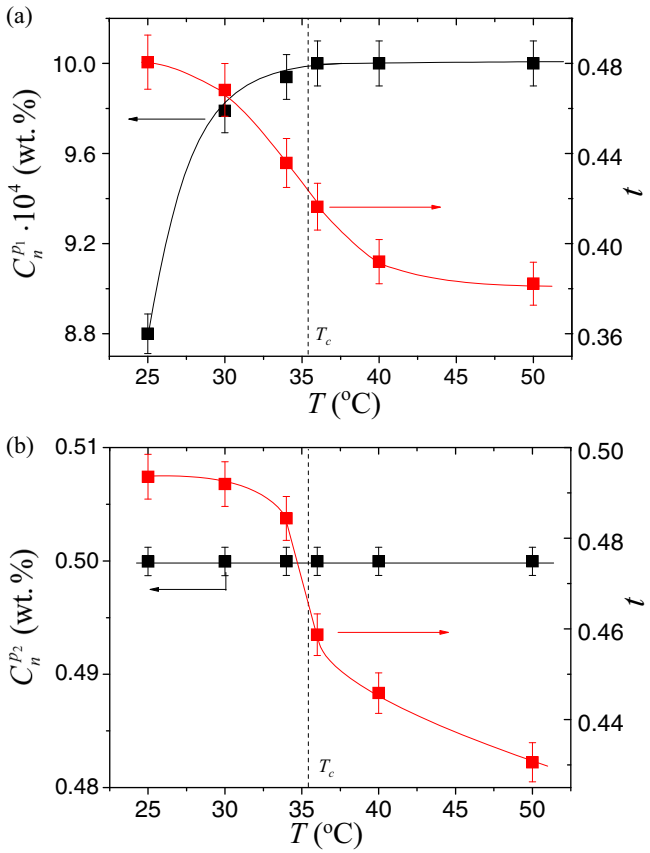

FIG. 4. (Color online) The percolation concentration C_n^p and the transport index t as the functions of temperature T for the first (a) and second (b) percolation stages. The dashed line represents the clearing temperature of LC 5CB, $T_c = 35.4°C$.

second processes as functions of temperature are presented in Figs. 4(a) and 4(b), respectively.

The first threshold concentration, $C_n^{p_1}$, approaches zero, because of the low viscosity of the LC. The transport index t for both transitions is lower than theoretical values for three-dimensional (3D) and even 2D percolation ($t = 2$ and $t = 4/3$, respectively [44]. As discussed in Ref. [43], this is due to strong aggregation of CNTs rather than a reduction in system dimensionality. In other words, an actual network is not a true statistical percolation derived by ignoring effective interaction of CNTs.

It can also be seen that the temperature dependencies of the first, $C_n^{p_1}$, and the second, $C_n^{p_2}$, threshold concentrations distinctly differ. At the first stage, the $C_n^{p_1}(T)$ curve grows in the nematic phase and reaches saturation in the isotropic phase. This implies that the liquid crystalline order imposed on CNTs promotes the interparticle contacts [32] and stabilizes the formed network. This is the important difference with the temperature behavior of percolating networks in the isotropic phase. In contrast, for the second percolation the concentration of percolation threshold $C_n^{p_2}$ practically does not change with a temperature T. At the same time, in both cases, the temperature affects the conductivity transport index t. This index drops with temperature increase, implying that the processes are slowed down.

To explain these results, we assume that the changes in percolation threshold concentration C_n^p indicate total destruction of network, while the index t reflects the strength of interparticle contacts. From this we can deduce that in the first percolation stage the LC host can significantly influence both the stability of the CNT network and the efficiency of the interparticle contacts. In turn, in the case of second percolation, the LC host does not affect the percolation point because of the high rigidity of the percolating network formed at this stage (due to the large number of interparticle contacts). Yet it may influence the strength of the contacts, obviously due to the dependence of the conduction of the LC intercalating layer on the phase state and temperature. Such an explanation suggests that even at the concentrations of a few wt.% CNTs interact with each other through the LC. Thus one can expect a new percolation step at a further increase of the concentration of CNTs, when the LC will be squeezed out from the interparticle contacts.

It may seem strange that the two percolations are not distinguishable in the case of series with a cell gap of 50 μm. The $\sigma(C_n)$ curve for this series can be satisfactorily fitted to a single curve [Eq. (2)] with the parameters $C_n^p = 0.003$ wt.% and $t = 0.86$. We believe that in this case two percolation processes strongly overlap so they manifest as a single hybrid percolation. A possible reason is that the sizes of the aggregates become comparable with a cell gap at much lower concentrations than in the case of 250-μm cells. This means that aggregates start to be compressed at a lower concentration. The facts that a threshold concentration appears between $C_n^{p_1}$ and $C_n^{p_2}$ and a scaling exponent t practically doubles compared with t_1 and t_2 in a two-step percolation confirm the assumption of a two-percolation processes.

The concentration dependence of the effective permittivity also shows interesting features. As shown in Ref. [14], the curves for thin cells ($d < 50$ μm) can be satisfactorily fitted to the scaling law described by Eq. (2). However, for the 250-μm series we observed a bend in the straight line $\epsilon'(C_n)$ obtained in a double logarithmic scale at a concentration roughly corresponding to $C_n^{p_2}$. This means that the effective permittivity of the composite is also sensitive to the second percolation of conductivity. We attribute this to an increase in polarizability of the percolating network with an improvment of electrical contacts between the nanotubes.

Finally, we propose a mathematical description for the observed two-step percolation based on various types of contacts between the particles. Previous research in this direction has been devoted exclusively to the polymers filled by CNTs. They assumed that the types of contacts between the conducting particles were distinct [26,45], there was a distribution of contact resistances for CNTs with different diameters [38], and there were local variations in particle concentration and/or shape and orientation [46].

Recently, the possibility of two-step percolation behavior for spherical particles was predicted by assuming the core-shell structure of conductive particles on the base of Bruggeman's effective medium approximation [23]. Further consideration is based on this approach. It is assumed that the observed two-step percolation in 5CB-CNT dispersions is caused by the core-shell structure of particles with highly conductive CNTs as cores and less conductive LC interfacial layers as shells.

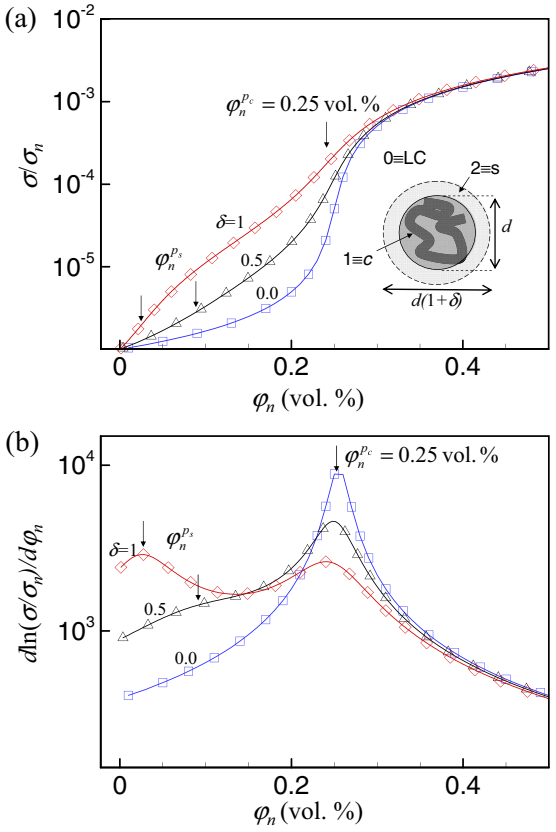

FIG. 5. (Color online) Relative electrical conductivity σ/σ_n (a) and its derivative $d\ln(\sigma/\sigma_n)/d\varphi_n$ (b) versus volume fraction of CNTs φ_n calculated for different values of parameter δ at $\varphi_n^{p_c} = 0.25$ vol.% (≈0.5 wt.%). The calculation was performed assuming that $\sigma_0/\sigma_n = 10^{-6}$ and $\sigma_s/\sigma_n = 10^{-3}$. The inset to (a) presents model of CNT coil with the core-shell structure.

Then the percolation thresholds $C_n^{p_1}$ and $C_n^{p_2}$ are associated with percolations through the shells and cores, respectively, and therefore will be further called C_n^s and C_n^c.

Taking into account the entangled state of CNTs, in further calculations they will be considered as quasispherical tortuous coils [47,48]. For the conductive spherical particles with a core-shell structure, Bruggeman's equation for electrical conductivity of a composite can be represented as [23]:

$$\sum_{i=0}^{2} \varphi_i \frac{\sigma_i - \sigma}{\sigma_i + A\sigma}, \tag{3}$$

where φ_i and σ_i are volume fraction and electrical conductivity, respectively, and A is an adjustable parameter determined by the value of percolation threshold and shape of the particle [49]. Index i for a continuous medium is 0 (σ_0,φ_0), for a particle core is 1 ($\sigma_1 = \sigma_n$, $\varphi_1 = \varphi_n$), and for a particle shell is 2 ($\sigma_2 = \sigma_s$, $\varphi_2 = \varphi_s$) [Fig. 5(a)].

For the compact spherical conductive inclusions analyzed in Ref. [23], A is 2 and the percolation threshold φ_1^p is 1/3. Note that modern phenomenological theory accounts also for the different critical exponents below and above the percolation threshold and estimates A as $(1-\varphi_1^p)/\varphi_1^p$ [50]. Numerous experimental data have shown that, for CNT filled composites,

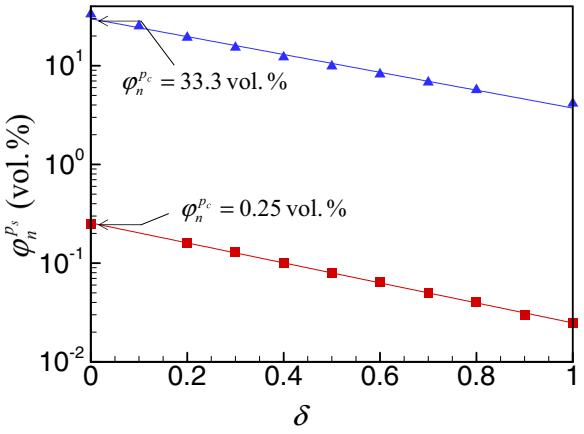

FIG. 6. (Color online) Exemplary dependencies of percolation concentration through shells, $\varphi_n^{p_s}$, versus relative width of the shell δ calculated for two different values of percolation concentration through cores, $\varphi_n^{p_c} = 0.25$ vol.% and $\varphi_n^{p_c} = 33.3$ vol.%. The calculations were performed assuming $\sigma_0/\sigma_n = 10^{-6}$ and $\sigma_2/\sigma_n = 10^{-3}$.

the value of φ_1^p may be extremely low, which may be explained by the giant aspect ratio of CNTs [20].

Dependence of $\sigma(\varphi)$ was obtained by solving Eq. (3) numerically, using $\Sigma\varphi_i = 1$, $\varphi_s = \varphi_n(1+\delta)^3$, and $\varphi_0 = 1 - \varphi_n - \varphi_n(1+\delta)^3$. Here δ is the relative enlargement of particle diameter $\Delta d/d$ due to the shell around the CNT and d is the effective diameter of the CNT coil [Fig. 5(a)]. It was also taken into account that $A = (1-\varphi_n^{p_c})/\varphi_n^{p_c}$, where $\varphi_n^{p_c}$ is the volume fraction of CNTs for percolation through the cores of the nanotubes [50].

Figure 5(a) presents examples of the calculated $\sigma/\sigma_n(\varphi_n)$ curves for different values of δ and $\varphi_n^{p_c} = 0.25$ vol.% (≈0.5 wt.%). The calculation were done using $\varphi_0/\varphi_n = 10^{-6}$, $\sigma_s/\sigma_n = 10^{-3}$. For the given value of the percolation threshold through cores $\varphi_n^{p_c}$, the percolation threshold through shells $\varphi_n^{p_s}$ may be identified as the maximum of the derivative $d\ln(\sigma/\sigma_n)/d\varphi_n$ [Fig. 5(b)].

The observed two steps reflect two sharp transitions of conductivity, $\sigma_0 \to \sigma_s$ and $\sigma_s \to \sigma$. Figure 6 presents examples of dependencies of percolation concentration of the first percolation threshold at $\varphi_n = \varphi_n^{p_s}$ (percolation through shells) versus the relative width of the shell δ at two different values of volume fraction $\varphi_n^{p_s}$ corresponding to percolation through cores.

The obtained data show that for thick shells ($\delta \approx 1$) the first percolation threshold, $\varphi_n^{p_s}$, can be noticeably smaller than the second one, $\varphi_n^{p_s}$, corresponding with our experimental observation.

V. CONCLUSION

The electrical conductivity and dielectric constant of CNTs dispersions in nematic LC 5CB has been studied within the dependence of CNT loading, cell thickness, and filling technique. The filling was based on capillary forces (C cells) or pressing the drop of dispersion between two substrates forming the cell (P cells). It was demonstrated that at high concentrations of CNTs ($C_n > 0.5$ wt%) the typical

LC technique of capillary filling becomes ineffective for LC dispersions of entangled CNTs. This happens when the thickness of the cell becomes comparable with the size of larger aggregates so only small aggregates or individual CNTs can be effectively involved by capillary forces inside the C cell. It results in selective sampling of CNTs at the edges of the C cell and lowering of actual concentration of CNTs in the cells comparing with that in the bulk, C_n. In this case, the true value of C_n in the cells provides only the pressing method. Understanding of this has made it possible to measure correctly the concentration dependencies of conductivity and effective permittivity of the dispersions in the wide range $C_n = 0$–2 wt.%. The corresponding dependence $\sigma(C_n)$ for the series of P samples with a thickness of 250 μm has clearly shown a two-stage percolation detected earlier only in polymer dispersions of CNTs [38]. Both percolation steps were fitted well to scaling percolation law. The first threshold concentration, $C_n^{p_1} \sim 10^{-4}$ wt.%, was sensitive to temperature and phase state of LC, while the second one, $C_n^{p_2} \sim 10^{-1}$ wt.%, remained practically unchanged in the temperature tests. The two-step percolation was described by using the mean-field formalism for the particles with a core-shell structure demonstrating various electrical conductivities of the cores and shells. The transition from the first to the second percolation can also be revealed for the corresponding $\epsilon'(C_n)$ curve if it is presented in a double logarithmic scale. This suggests that both conductivity and polarizability of the composites are sensitive to the second percolation of CNTs. The observed two-stage formation of the CNT network opens rather interesting research prospects. Since the stabilizing role of the nematic phase for the particle network has been discovered (especially at the first stage of its formation), it is rather interesting to clarify the effect of other LC phases on the network formation. Besides, as for other characteristics of the studied system, the percolation features can be drastically affected by LC- CNT interfacial interaction [51,52], introduction of additional particles [14], and curing of the samples in external fields [8,16,17]. Finally, we expect new peculiarities in electro-optic and magneto-optic responses, associated with the two-stage nature of nanoparticle percolation.

ACKNOWLEDGMENTS

This work was partially funded under Project No. 2.16.1.4 (NAS of Ukraine). The authors thank Cheap Tubes for providing the samples of short nanotubes involved in this research.

[1] A. S. Brady-Estevez, M. H. Schnoor, C. D. Vecitis, N. B. Saleh, and M. Elimelech, Langmuir **26**, 14975 (2010).
[2] M. Endo, M. Strano, and P. Ajayan, Top. Appl. Phys. **111**, 13 (2008).
[3] T. Hasan, Z. Sun, F. Wang, F. Bonaccorso, P. Tan, A. Rozhin, and A. Ferrari, Adv. Mater. **21**, 3874 (2009).
[4] G. Pandey and E. Thostenson, Polym. Rev. **52**, 355 (2012).
[5] F. Valentini, M. Carbone, and G. Palleschi, Anal. Bioanal. Chem. **405**, 451 (2013).
[6] C. Zakri, Liq. Cryst. Today **16**, 1 (2007).
[7] O. Trushkevych, N. Collings, T. Hasan, V. Scardaci, A. C. Ferrari, T. D. Wilkinson, W. A. Crossland, W. I. Milne, J. Geng, B. F. G. Johnson, and S. Macaulay, J. Phys. D **41**, 125106 (2008).
[8] L. Dolgov, O. Kovalchuk, N. Lebovka, S. Tomylko, and Yaroshchuk, in *Carbon Nanotubes*, edited by J. M. Marulanda (In-Tech, Vukovar, Croatia, 2010), pp. 451–483.
[9] R. Basu, Dielectric studies of nanostructures and directed self-assembled nanomaterials in nematic liquid crystals, Ph.D. thesis, Worcester Polytechnic Institute, Worcester, MA, 2010.
[10] G. Scalia, ChemPhysChem **11**, 333 (2010).
[11] I. Dierking, G. Scalia, P. Morales, and D. LeClere, Adv. Mater. **16**, 865 (2004).
[12] P. van der Schoot, V. Popa-Nita, and S. Kralj, J. Phys. Chem. B **112**, 4512 (2008).
[13] M. Rahman and W. Lee, J. Phys. D **42**, 063001 (2009).
[14] O. Yaroshchuk, S. Tomylko, O. Kovalchuk, and N. Lebovka, Carbon **68**, 389 (2014).
[15] R. Basu and G. Iannacchione, Appl. Phys. Lett. **93**, 183105 (2008).
[16] L. Dolgov, O. Yaroshchuk, and M. Lebovka, Mol. Cryst. Liq. Cryst. **496**, 212 (2008).
[17] L. Dolgov, O. Yaroshchuk, S. Tomylko, and N. Lebovka, Condens. Matter Phys. **15**, 33401 (2012).
[18] L. Dolgov, N. Lebovka, and O. Yaroshchuk, Colloid J. **71**, 603 (2009).
[19] O. Yaroshchuk, S. Tomylko, L. Dolgov, T. Semikina, and O. Kovalchuk, Diam. Relat. Mater. **19**, 567 (2010).
[20] W. Bauhofer and J. Z. Kovacs, Compos. Sci. Technol. **69**, 1486 (2009).
[21] M. Sahimi, Phys. Rep. **306**, 213 (1998).
[22] C. Calberg, S. Blacher, F. Gubbels, F. Brouers, R. Deltour, and R. Jérôme, J. Phys. D **32**, 1517 (1999).
[23] M. Sushko and A. Semenov, Condens. Matter Phys. **16**, 13401 (2013).
[24] J. O. Aguilar, J. R. Bautista-Quijano, and F. Avilés, Express Polym. Lett. **4**, 292 (2010).
[25] M. Zhang, G. Yu, H. Zeng, H. Zhang, and Y. Hou, Macromolecules **31**, 6724 (1998).
[26] B. Nettelblad, E. Martensson, C. Onneby, U. Gafvert, and A. Gustafsson, J. Phys. D **36**, 399 (2003).
[27] J. Z. Kovacs, R. E. Mandjarov, T. Blisnjuk, K. Prehn, M. Sussiek, J. Müller, K. Schulte, and W. Bauhofer, Nanotechnology **20**, 155703 (2009).
[28] R. Haggenmueller, H. Gommans, A. Rinzler, J. Fischer, and K. Winey, Chem. Phys. Lett. **330**, 219 (2000).
[29] A. Behnam, J. Guo, and A. Ural, J. Appl. Phys. **102**, 044313 (2007).
[30] A. Behnam and A. Ural, Phys. Rev. B **75**, 125432 (2007).
[31] A. Dombovari, N. Halonen, A. Sapi, M. Szabo, G. Toth, J. Mäklin, K. Kordas, J. Juuti, H. Jantunen, A. Kukovecz, and Z. Konya, Carbon **48**, 1918 (2010).
[32] F. Du, J. E. Fischer, and K. I. Winey, Phys. Rev. B **72**, 121404 (2005).

[33] E. S. Choi, J. S. Brooks, D. L. Eaton, M. S. Al-Haik, M. Y. Hussaini, H. Garmestani, D. Li, and K. Dahmen, J. Appl. Phys. **94**, 6034 (2003).
[34] L. J. Lanticse, Y. Tanabe, K. Matsui, Y. Kaburagi, K. Suda, M. Hoteida, M. Endo, and E. Yasuda, Carbon **44**, 3078 (2006).
[35] A. V. Koval'chuk, L. Dolgov, and O. Yaroshchuk, Semiconductor Phys. Quant. Electron. Optoelectron. **11**, 337 (2008).
[36] A. I. Goncharuk, N. I. Lebovka, L. N. Lisetski, and S. S. Minenko, J. Phys. D **42**, 165411 (2009).
[37] N. Lebovka, T. Dadakova, L. Lysetskiy, O. Melezhyk, G. Puchkovska, T. Gavrilko, J. Baran, and M. Drozd, J. Molec. Struct. **887**, 135 (2008).
[38] J. Z. Kovacs, B. S. Velagala, K. Schulte, and W. Bauhofer, Compos. Sci. Technol. **67**, 922 (2007).
[39] A. V. Melezhik, Y. I. Sementsov, and V. V. Yanchenko, Russ. J. Appl. Chem. **78**, 917 (2005).
[40] L. N. Lisetski, S. S. Minenko, V. V. Ponevchinsky, M. S. Soskin, A. I. Goncharuk, and N. I. Lebovka, Mater. Sci. Eng. Technol. **42**, 5 (2011).
[41] J. Deschamps, J. P. M. Trusler, and G. Jackson, J. Phys. Chem. B **112**, 3918 (2008).
[42] H. Pang, C. Chen, Y. Bao, J. Chen, X. Ji, J. Lei, and Z.-M. Li, Mater. Lett. **79**, 96 (2012).
[43] J. Sandler, J. Kirk, I. Kinloch, M. Shaffer, and A. Windle, Polymer **44**, 5893 (2003).
[44] D. Stauffer and A. Aharony, *Introduction to Percolation Theory* (Taylor & Francis, London, 1992).
[45] P. Sheng and R. V. Kohn, Phys. Rev. B **26**, 1331 (1982).
[46] D. McQueen, K.-M. Jager, and M. Pelskova, J. Phys. D **37**, 2160 (2004).
[47] H. S. Lee, in *Nanotechnology and Nanomaterials*, edited by S. Suzuki (In-Tech, Vukovar, Croatia, 2013) p. 3953.
[48] L. N. Lisetski, A. P. Fedoryako, A. N. Samoilov, S. S. Minenko, M. S. Soskin, and N. I. Lebovka, Eur. Phys. J. E: Soft Matter **37**, 24 (2014).
[49] W.-Z. Cai, S.-T. Tu, and J.-M. Gong, J. Comp. Mater. **40**, 2131 (2006).
[50] D. S. McLachlan and G. Sauti, J. Nanomater. **2007**, 30389 (2007).
[51] V. Popa-Nita, I. Gerlič, and S. Kralj, Int. J. Molec. Sci. **10**, 3971 (2009).
[52] V. Popa-Nita and S. Kralj, J. Chem. Phys. **132**, 024902 (2010).